

Atomistic simulations of low-density nanoporous materials: Carbon nanofoams

C. Mathioudakis and P. C. Kelires

Research Unit for Nanostructured Materials Systems, Department of Mechanical and Materials Science Engineering, Cyprus University of Technology, P.O. Box 50329, 3603 Limassol, Cyprus

(Received 14 November 2012; revised manuscript received 21 April 2013; published 8 May 2013)

Atomistic simulations give new insights into the properties of carbon nanofoams, a low-density nanoporous and nanostructured material. It is shown that agglomeration, crosslinking, and deformation, processes that are often ignored in theoretical descriptions of nanomaterials, have a dramatic effect on their properties. A most striking finding is that nanofoams composed exclusively of semiconducting nanostructures turn out to be metallic with high conductivity and optical absorptance. The underlying mechanism may explain relevant observations in other nanoporous materials. The simulated structures contain trivalent carbon atoms, suggested earlier to be a major source of magnetism in these materials.

DOI: [10.1103/PhysRevB.87.195408](https://doi.org/10.1103/PhysRevB.87.195408)

PACS number(s): 73.22.-f, 61.43.Bn, 61.43.Gt

I. INTRODUCTION

While the denser forms of carbon, ranging from graphitelike to diamondlike manifestations, are extensively studied and well understood, the ultra-low-density forms remain largely unknown and unexplored. In this density regime, nanoporous formation along with nanostructuring and coexistence of various carbon hybridizations give rise to three-dimensional (3D) structures with outstanding properties.

In such low-density nanostructured materials, it is crucial to understand the nature of the interfaces, especially how the constituent units interact and link to each other. This factor is often ignored, and properties are inferred or projected by just studying the ideal fundamental units and/or periodic arrangements of them. However, this approach does not capture many of the aspects of the real 3D material. The process during which nanostructures agglomerate and crosslink neither yields periodic arrangements nor sustains ideal, unmodified units.

Here, we show that the proper atomistic description of nanoporous materials, by fully incorporating the interactions among nanostructures and the interface factor, may dramatically alter this simplistic view and the conclusions emanating from it. For example, we show that nanostructures which are known to be semiconducting may crosslink to yield a 3D nanomaterial that is not semiconducting, but instead highly conductive.

We demonstrate these ideas by studying, exploring, and predicting the properties of carbon nanofoams (CNFs). These are random structures resembling a foam, characterized by an open, weblike network with a large surface area and high porosity. Their mass density can be very low, reaching values of the order of mg/cm^3 .^{1,2} They are produced by methods such as laser ablation,¹ cluster beam deposition (spongy carbon),³ pyrolysis (nanoporous carbon),^{4,5} and sol-gel methods.⁶ Interest in them steadily increases because of promising applications, such as in catalysis, tribology, and energy storage, and after reports of intrinsic magnetism.^{2,7}

CNFs produced by laser ablation¹ have a nanostructured network composed of randomly interconnected clusters with medium-range order correlations.² The constituent units in this and other types of foams prepared by alternative methods^{3,8} are found to be graphitelike hyperbolic nanostructures having negative Gaussian curvature, called schwarzites.⁹ However,

the microstructure of these networks, especially how these units are linked to each other, is far from being well understood. Foams made up of carbon nanotubes (CNTs) have also been reported.¹⁰ Previous theoretical studies mainly focused on the properties of isolated or periodic constituent units.^{5,7,11,12}

An outstanding finding of our atomistic simulations is that bulk CNFs composed of semiconducting units are metallic with high conductivity, having no localized π states near the Fermi level. This effect solely arises from the entanglement, linking, and modification of the nanostructures during agglomeration.

The paper is organized as follows. In the next section, the Monte Carlo and tight-binding methods used to construct and extract the properties of CNFs are described. In Sec. III, the results and the associated discussion are given. Conclusions and prospects for extending our approach to other low-density carbon nanomaterials are discussed in Sec. IV.

II. METHODOLOGY

We construct the CNF networks in two steps: we first condense a “vapor” containing various schwarzite units at large distances, using Monte Carlo (MC) simulations in the (N, P, T) isothermal-isobaric ensemble, at 1000 K and under various pressures. The energetics are described by the Tersoff empirical potential.¹³ We use cubic supercells of ~ 700 and ~ 1600 carbon atoms, depending on the type and number of units, with periodic boundary conditions. The units used here are representative of a large family of schwarzite structures with different topological genus, surface, type of nonhexagonal rings, and electronic structure, and are shown in Fig. 1. These are the C_{168} structure (a semiconducting D7 graphite surface with 168 C atoms curved by the introduction of heptagons),¹¹ as well as 192-atom structures based on the semiconducting P8 and metallic G8 surfaces curved by octagons.^{14,15} During condensation, the units approach each other, agglomerate, and interlink with some degree of fragmentation, which induces disorder around the junctions and curvature alterations on the surfaces. The resulting networks are then relaxed at 300 K.

In the second step, the MC-prepared CNF networks are fully relaxed using tight-binding molecular dynamics (TBMD) simulations in the (N, V, T) canonical ensemble. This proceeds

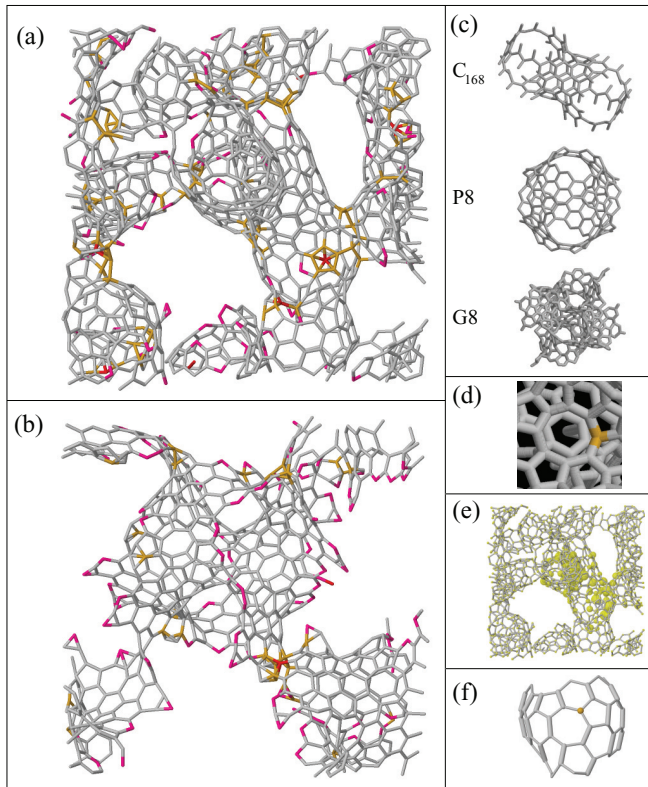


FIG. 1. (Color online) (a, b) Models of CNF networks, with periodic boundary conditions, composed of C_{168} and G8 units, respectively. Grey, orange, and magenta denote sp^2 , sp^3 , and sp^1 bonding, respectively. (c) The three schwarzite fundamental units used in this work. (d) An eight-membered ring in a C_{168} CNF. An atom with significant contribution to the electronic density of states (EDOS) at the Fermi level is highlighted. (e) Site contributions to the wave function of a π state at the Fermi level in the CNF of panel (a). (f) A trivalent carbon atom in a heptagon. Thin and thick sticks denote single and double bonds, respectively.

by extensive annealing at 2000 K and then relaxation of the volume/density at 300 K, where structural, mechanical, and optoelectronic properties are inferred. The calculations are carried out within the TB framework developed at the Naval Research Laboratory (NRL).¹⁶ This is a nonorthogonal model, using distance- and environment-dependent parameters for transferability between different structures. The successful description of amorphous/disordered phases of carbon by this model was previously demonstrated.¹⁷

III. RESULTS AND DISCUSSION

We first begin with the microstructure of CNFs. Figures 1(a) and 1(b) show two representative, fully relaxed CNF networks with densities 0.8 and 0.5 g/cm³, constructed from C_{168} and G8 units, respectively.¹⁸ The nanoporous nature of both structures is evident. The main characteristic is that the randomly interacting and interlinked units do not remain intact, preserving their shape and ideal surface curvature, but they are deformed, sometimes fragmented, which results in the appearance of non- sp^2 atoms and the formation of new, large atomic rings. These have a profound effect on the electronic properties, as shown below.

The fraction of the generated sp^3 sites in these networks is $\sim 5\%$. Many of them are linking geometries at the junctions between the units, where extensive rearrangements and rebonding occur. It is quite interesting that sp^3 sites are formed at such low densities. In amorphous carbon (a-C), no sp^3 sites are found below ~ 1.3 g/cm³.¹⁹ This might be the result of the generated local pressure at the interacting regions. However, the interfaces contain also, as linking geometries, both sp^2 and sp^1 sites. The latter sites, found in pairs and chained geometries, have a total fraction of $\sim 7\%$ in C_{168} CNF and $\sim 10\%$ in P8 and G8 CNF. The new, large atomic rings are generated due to surface deformation when certain rings are broken and then reformed. These are usually eight- and nine-membered rings. Figure 1(d) shows such an eight-membered ring in a C_{168} CNF. We also find five-membered rings in our structures, in agreement with findings of an earlier random schwarzite model.²⁰

Figure 2 shows the reduced radial distribution functions $G(r)$ of CNF networks compared to the $G(r)$ of a low-density a-C network, generated with the same TBMD methodology. There are some striking differences between them. One is the feature between the second and third peak, at ~ 2.8 Å. This extra peak corresponds to in-plane distances in graphite and is absent in a-C. Another notable difference is that the fourth and fifth peaks in CNF remain intense, while they are much weaker in a-C. These differences show that medium-range order correlations are preserved in CNFs, in agreement with experiment,² while they are absent in a-C. We conclude that CNFs are not plausible models or ingredients of low-density a-C, as suggested earlier,^{11,20} although they have other common features, such as the presence of numerous sp^1 sites.^{19,21–23}

Unfortunately, no $G(r)$ diffraction analysis for the foams of Refs. 1 and 2 exists for direct comparison. Our analysis fills this gap and also clarifies the issue about the extent of the sp^3 fraction in these foams. This was initially reported,^{1,2} through electron-energy-loss spectroscopy analysis, to be very high (35% on average and up to 60% in some regions). This

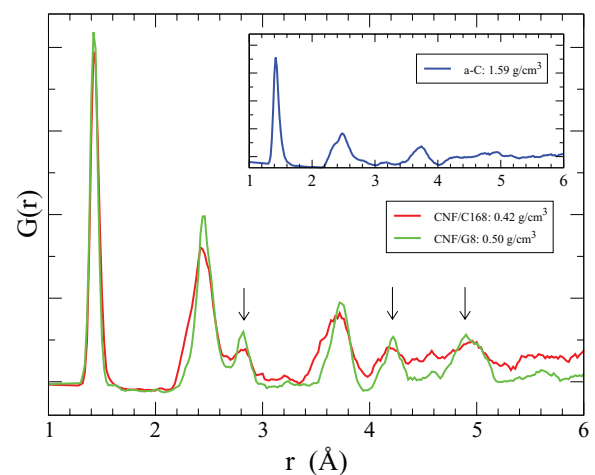


FIG. 2. (Color online) Reduced radial distribution functions $G(r)$ of C_{168} and G8 foams. Arrows denote intense peaks indicative of medium-range order. The inset shows the $G(r)$ of a low-density a-C network.

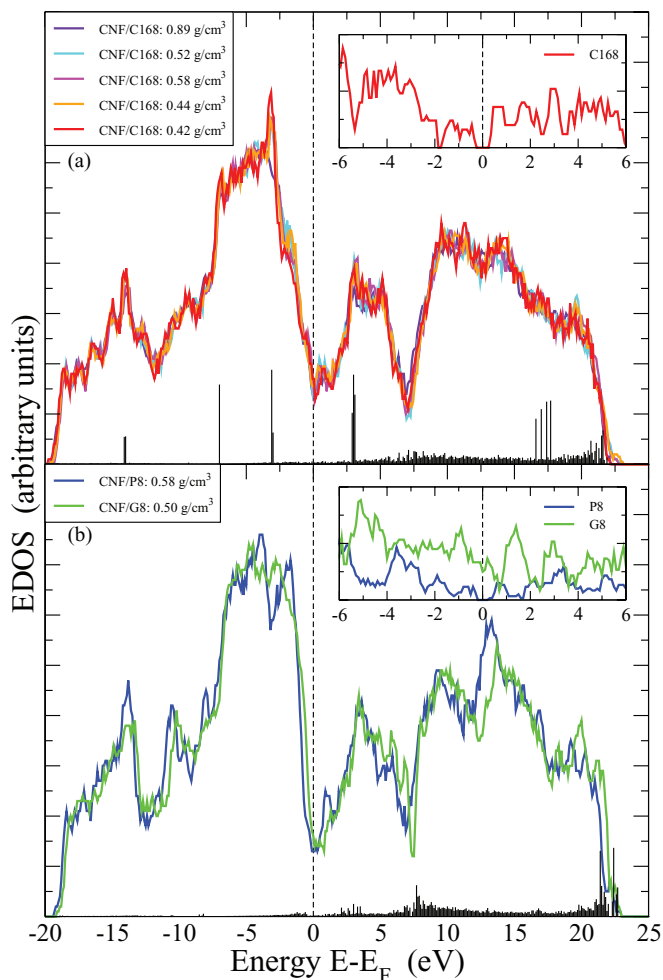


FIG. 3. (Color online) (a) EDOS of C_{168} CNFs with various densities. Vertical lines indicate a typical distribution of localized states from inverse participation ratio (IPR) analysis. The inset shows the EDOS of the periodic C_{168} structure. (b) EDOS of P8 and G8 CNFs and the localized states. The inset shows the EDOS of the respective periodic structures.

must be an overestimation.^{24,25} Such a high sp^3 content would cause a shift in the position of the first peak in the $G(r)$ toward diamondlike values, or its split into two subpeaks. Indeed, from a subsequent analysis of these foams by ^{13}C NMR measurements,²⁶ one infers reliable estimates of sp^3 and sp^1 fractions ($\sim 8\%$ and 16% , respectively), in good agreement with our values.

Despite their disordered character, the CNF models have energies comparable to a-C, well known to be a quite stable phase. On average, their formation energies are 0.5–0.8 eV/atom relative to an ideal graphene plane. Thus, CNFs are energetically stable and feasible in the bulk form studied here, representing thin films deposited on suitable substrates with good adhesion.

Having elucidated the microstructure of CNFs, we now proceed to the study of the electronic structure of CNFs. Figure 3(a) plots the calculated TB EDOS of various C_{168} CNFs with different densities. The striking finding is that in all cases these CNFs have no energy gap, since the region around the Fermi level ϵ_F is filled with π states, suggesting

metalliclike behavior. This is in contrast to the case of the C_{168} periodic structure which is semiconducting, having a clear gap of ~ 0.8 eV with the present TB scheme and in agreement with previous studies,²⁷ as shown in the inset of Fig. 3(a). The opening of a gap in certain schwarzite structures has been attributed to the misalignment of the π orbitals due to the curvature induced by the odd-membered rings.²⁷ This is similar to the opening of the π - π^* gap in a-C due to misaligned π orbitals in neighboring sp^2 sites.²⁴

We unravel the origin of this surprising result, i.e., having 3D metallic foams totally composed of semiconducting nanostructures, by further analyzing the EDOS of CNFs into atomic contributions. We find that many atoms contributing significantly at ϵ_F are sp^2 -bonded atoms located at large eight- and nine-membered rings formed during the CNF agglomeration. Such a site in an eight-membered ring is highlighted in Fig. 1(d). This suggests that the introduction of large aromatic rings alters the curvature locally into a more planar geometry, causing the proper alignment of π orbitals and thus closing the gap. Equally interesting is that atoms in the seven-membered rings, inducing the negative curvature in the original structure, and even atoms in the majority six-membered rings, do contribute states at ϵ_F after the crosslinking, but not as strongly as atoms in the larger rings. These effects show that properties of nanostructured materials cannot always be extrapolated from those of the respective constituent ideal units.

As a result of these curvature modifications, the π and π^* states near ϵ_F are delocalized. An IPR analysis²⁸ shows that the ϵ_F region is practically free of localized states, as seen in Fig. 3(a). The extent of delocalization is demonstrated in Fig. 1(e), showing that such π states are spatially extended over several schwarzite units. This is in sharp contrast to a-C, where the π and π^* states near ϵ_F are localized, causing the low conductivity of the material.²⁴ It also confirms the aromatic nature of these states in CNFs. The IPR analysis shows that there are localized states, mainly at sp^1 sites at the internal surfaces, but these lie deeper in the valence and conduction bands. A direct experimental evidence for delocalized π states in CNFs prepared by laser ablation is provided by electron paramagnetic resonance measurements.²⁹

Examining CNFs formed from other types of schwarzite units, or a mixture of them, we always find gapless systems. This is demonstrated in Fig. 3(b), which shows the EDOS of P8 and G8 CNFs. Note that the periodic P8 structure is semiconducting while the G8 is metallic, as shown in the inset of Fig. 3(b) and in agreement with previous studies.¹² As in the C_{168} CNF case, the P8 CNFs are made metallic because of curvature modifications throughout the network, especially due to seven- and nine-membered rings not present before crosslinking. The gapless nature of the G8 unit does not necessarily mean that a metallic character is *a priori* imposed on the foam, given the substantial modifications during foam formation. Yet, despite that the shape of the π bands has changed in the G8-to-G8-CNF process, the resulting foam is gapless with no localized states at ϵ_F . We conclude that the gapless character of CNFs is a global phenomenon, irrespective of the electronic structure of the constituent units, and is attributed to the altering of local surface curvature during agglomeration.

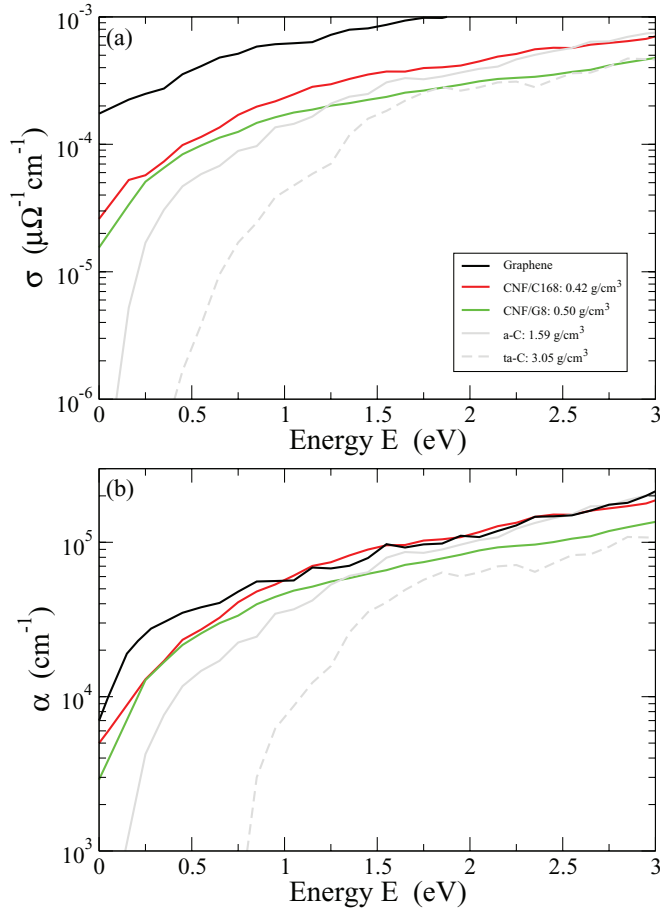


FIG. 4. (Color online) (a) Conductivity of two representative foams compared to that of a graphene layer, of a low-density a-C cell, and of a tetrahedral a-C cell. (b) Optical absorption of the above materials.

The delocalized nature of π states in CNFs is also confirmed by calculating the electrical conductivity of various cells. This is given in its standard frequency-dependent form by

$$\sigma(\omega) = \left(\frac{2\pi e^2}{3V\hbar^2\omega} \right) \sum_{i,f} (E_f - E_i)^2 |\langle f|\mathbf{r}|i\rangle|^2 \times \delta(E_f - E_i - \hbar\omega), \quad (1)$$

where the Harrison approximation for the momentum matrix elements,³⁰ $\hbar\langle f|\mathbf{P}|i\rangle = \text{Im}(E_f - E_i)\langle f|\mathbf{r}|i\rangle$, has been utilized. (Equivalently, conductivity can be expressed in a similar energy-dependent form.) The dc conductivity is obtained in the limit ω (or E) \rightarrow 0.

The results are given in Fig. 4(a). We compute, on average, a dc conductivity σ_{dc} of CNFs of the order of $10^{-5} \mu\Omega^{-1} \text{cm}^{-1}$. This is three to four orders of magnitude higher than the well-established values of σ_{dc} of sp^2 -rich graphitelike a-C, and more than eight orders of magnitude higher than sp^3 -rich tetrahedral a-C (ta-C).³¹ Our computed values are $\sim 10^{-8} \mu\Omega^{-1} \text{cm}^{-1}$ for the former and practically zero for the latter. The σ_{dc} of CNFs is comparable with the σ_{dc} of graphite (10^{-3} – $10^{-5} \mu\Omega^{-1} \text{cm}^{-1}$),³² that of CNT foams ($\sim 10^{-4} \mu\Omega^{-1} \text{cm}^{-1}$),¹⁰ and with our calculated value of $\sim 2 \times 10^{-4} \mu\Omega^{-1} \text{cm}^{-1}$ for a graphene layer, which

agrees with several experimental measurements in graphene materials.³³

The laser-ablated CNFs were, on the other hand, reported to be semiconducting.^{1,2} This seems to contradict the finding of delocalized π states in these foams.²⁹ Since a high fraction of sp^3 sites, able to inhibit conduction, is excluded,²⁶ a plausible explanation is that these CNFs, due to their extremely low density, become floppy,³⁴ with a partial loss of cluster connectivity and percolation. This interrupts the conduction of the delocalized π states across the system.³⁵ Our networks possess full connectivity and percolation. Floppiness might also explain the gradual loss of magnetization in the CNFs of Ref. 2.

Our theory of π -electron delocalization may explain the enhanced conductivity observed in other nanoporous systems, such as in CNT foams. These are reported¹⁰ to be based on carbon aerogels as a binding material in which single-wall CNTs are randomly dispersed. The drastic enhancement observed with increasing CNT content cannot be explained by the mere presence of CNTs alone, since a random mixture of both metallic and semiconducting tubes would unavoidably limit the conductivity. Thus, the only way to have enhanced conductivity in such a system is the transformation of a large fraction of the semiconducting units into metallic ones, through curvature modifications.

The CNFs are also highly absorptive, as demonstrated in Fig. 4(b). The absorption coefficient of various cells, given by $\alpha(\omega) = \frac{\omega\epsilon_2(\omega)}{nc}$, where $\epsilon_2(\omega)$ is the imaginary part of the dielectric function and n is the refractive index of the material,³⁶ reveals that their absorptance is similar to a graphene layer and considerably higher than that of low-density a-C and, especially, ta-C. The strong absorption makes CNFs promising materials for optical applications.

A direct link to the laser-ablated CNFs² is provided by our finding of sterically protected radicals (trivalent carbon atoms). These were suggested⁷ to be a major source of intrinsic magnetism in CNFs, introducing unpaired electrons (spins). A representative radical in our models is shown in Fig. 1(f). The radicals are all associated with heptagons,⁷ but these may also neighbor pentagons and not just hexagons, as in the ideal schwarzite tetrapod structure of Ref. 7. We find two to three radicals in every generated network, in agreement with experiment² (one unpaired spin in every 300 carbon atoms). Of course, the detailed study of magnetism in such materials is beyond the scope of the present work and requires further investigations.

Finally, we address the issue of the mechanical stability of CNFs. In principle, if we ignore pore formation, these networks should not be floppy but rigid, since their average coordination number ranges from 2.7 to 2.9. It is thus higher than the critical coordination of 2.4 at which the rigid-to-floppy transition takes place, according to mean-field theory³⁷ and TB calculations.¹⁹ However, the presence of pores suggests possible deviations from such continuous random network considerations. Still, our calculations of the bulk modulus of various CNF networks, at the densities considered here, show that the structures are rigid. We compute bulk moduli in the range 5–20 GPa.³⁸ This is much lower than values for typical 3D carbon materials (e.g., a-C) but still high enough to make CNFs durable for potential applications. CNFs with lower densities and larger pores¹⁸

are expected to have even smaller moduli, and at a critical density (presently unknown) they become floppy³⁷ and lose connectivity, as most likely is the case³⁴ with the laser-ablated CNFs.^{1,2} Producing more rigid CNF films in the laboratory, by optimizing their density, is desirable.

IV. CONCLUSIONS

In conclusion, our computational studies showed that the properties of realistic CNF networks are strongly influenced by the process of agglomeration and crosslinking of the constituent nanostructures. We found that rigid CNFs are characterized by strong medium-range order, contain a small fraction of sp^3 sites, and are metallic with high conductivity and optical absorptance. We also found, for the first time, direct evidence for the existence of carbon radicals in CNFs. The mechanism for the enhanced conductivity of carbon

nanofoams may serve as a model for any type of low-density material made of randomly interconnected nanostructures, such as carbon nanotubes and graphene nanoribbons. These are expected to have positive Gaussian curvature and thus different microstructure and medium-range order compared to the negatively curved CNFs. Work towards this direction is in progress.

ACKNOWLEDGMENTS

This work is supported by the Strategic Infrastructure Project NEW INFRASTRUCTURE/ΣTPATH/0308/04 of DESMI 2008, which is co-financed by the European Regional Development Fund, the European Social Fund, the Cohesion Fund, and the Research Promotion Foundation of the Republic of Cyprus. Discussions with John Giapintzakis are gratefully acknowledged.

-
- ¹A. V. Rode, S. T. Hyde, E. G. Gamally, R. G. Elliman, D. R. McKenzie, and S. Bulcock, *Appl. Phys. A* **69**, S755 (1999); A. V. Rode, E. G. Gamally, and B. Luther-Davies, *ibid.* **70**, 135 (2000).
- ²A. V. Rode, E. G. Gamaly, A. G. Christy, J. G. FitzGerald, S. T. Hyde, R. G. Elliman, B. Luther-Davies, A. I. Veinger, J. Androulakis, and J. Giapintzakis, *Phys. Rev. B* **70**, 054407 (2004).
- ³E. Barborini, P. Piseri, P. Milani, G. Benedek, C. Ducati, and J. Robertson, *Appl. Phys. Lett.* **81**, 3359 (2002).
- ⁴V. Petkov, R. DiFrancesco, J. Billinge, M. Acharya, and H. Foley, *Philos. Mag.* **B 79**, 1519 (1999).
- ⁵J. M. Carlsson and M. Scheffler, *Phys. Rev. Lett.* **96**, 046806 (2006).
- ⁶C. Moreno-Castilla and F. J. Maldonado-Hódar, *Carbon* **43**, 455 (2005).
- ⁷N. Park, M. Yoon, S. Berber, J. Ihm, E. Osawa, and D. Tomaneck, *Phys. Rev. Lett.* **91**, 237204 (2003).
- ⁸D. Donadio, L. Colombo, P. Milani, and G. Benedek, *Phys. Rev. Lett.* **83**, 776 (1999).
- ⁹H. A. Schwarz, *Gesammelte Mathematische Abhandlungen*, Vols. 1 and 2 (Springer, Berlin, 1890).
- ¹⁰M. Worsley, S. O. Kucheyev, J. H. Satcher, A. V. Hamza, and T. F. Baumann, *Appl. Phys. Lett.* **94**, 073115 (2009).
- ¹¹D. Vanderbilt and J. Tersoff, *Phys. Rev. Lett.* **68**, 511 (1992).
- ¹²F. Valencia, A. H. Romero, E. Hernández, M. Terrones, and H. Terrones, *New J. Phys.* **5**, 123 (2003).
- ¹³J. Tersoff, *Phys. Rev. Lett.* **61**, 2879 (1988).
- ¹⁴A. L. Mackay and H. Terrones, *Nature (London)* **355**, 762 (1991).
- ¹⁵H. Terrones and A. L. Mackay, *Carbon* **30**, 1251 (1992).
- ¹⁶D. A. Papaconstantopoulos and M. J. Mehl, *J. Phys. Condens. Matter* **15**, R413 (2003).
- ¹⁷M. G. Fyta, I. N. Remediakis, P. C. Kelires, and D. A. Papaconstantopoulos, *Phys. Rev. Lett.* **96**, 185503 (2006).
- ¹⁸Networks with lower densities and larger pores, comparable to experimental values, can in principle be achieved with the MC method; however, this requires much larger computational cells, of the order of several thousands of atoms, which are intractable by the TBMD method.
- ¹⁹C. Mathioudakis, G. Kopidakis, P. C. Kelires, C. Z. Wang, and K. M. Ho, *Phys. Rev. B* **70**, 125202 (2004).
- ²⁰S. J. Townsend, T. J. Lenosky, D. A. Muller, C. S. Nichols, and V. Elser, *Phys. Rev. Lett.* **69**, 921 (1992).
- ²¹D. G. McCulloch, D. R. McKenzie, and C. M. Goringe, *Phys. Rev. B* **61**, 2349 (2000).
- ²²U. Stephan, T. Frauenheim, P. Blaudeck, and G. Jungnickel, *Phys. Rev. B* **50**, 1489 (1994).
- ²³A. Merchant, D. McCulloch, D. McKenzie, Y. Yin, L. Hall, and E. Gerstner, *J. Appl. Phys.* **79**, 6914 (1996).
- ²⁴J. Robertson, *Mater. Sci. Eng., R* **37**, 129 (2002).
- ²⁵Electron-energy-loss spectroscopy overestimates the sp^3 content because it neglects the sp^1 sites, mingling them with the sp^2 sites.
- ²⁶R. Blinc, P. Cevc, D. Arcon, B. Zalar, A. Zorko, T. Apih, F. Milia, N. Madsen, A. Christy, and A. Rode, *Phys. Status Solidi B* **243**, 3069 (2006).
- ²⁷R. Phillips, D. A. Drabold, T. Lenosky, G. B. Adams, and O. F. Sankey, *Phys. Rev. B* **46**, 1941 (1992).
- ²⁸The IPR is defined as $P = \sum_i c_i^4$, where c_i are the coefficients in the expansion of the eigenstates in terms of the local orbitals, and it is a measure of the localization of the electronic states.
- ²⁹D. Arcon, Z. Jagličič, A. Zorko, A. V. Rode, A. G. Christy, N. R. Madsen, E. G. Gamaly, and B. Luther-Davies, *Phys. Rev. B* **74**, 014438 (2006).
- ³⁰W. A. Harrison, *Elementary Electronic Structure* (World Scientific, Singapore, 1999), p. 219.
- ³¹S. R. P. Silva, in *Handbook of Thin Film Materials*, edited by H. S. Nalwa, Vol. 4 (Academic, New York, 2002), p. 403.
- ³²N. Deprez and D. S. McLachlan, *J. Phys. D: Appl. Phys.* **21**, 101 (1988).
- ³³S. Stankovich, D. Dikin, R. Piner, K. Kohlhaas, A. Kleinhammes, Y. Jia, Y. Wu, S. Nguyen, and R. Ruoff, *Carbon* **45**, 1558 (2007); H. Chen, M. Muller, K. Gilmore, G. Wallace, and D. Li, *Adv. Mater.* **20**, 3557 (2008); Z. Wu, W. Ren, L. Gao, J. Zhao, Z. Chen, B. Liu, D. Tang, B. Yu, C. Jiang, and H. Cheng, *ACS Nano* **3**, 411 (2009).
- ³⁴The floppy character of the CNFs of Ref. 2 is confirmed by J. Giapintzakis (private communication); the samples were very easily deformed and stripped from the substrates.

³⁵Percolation theory predicts that conductivity drops rapidly when approaching the percolation threshold, related here to the degree of cluster connectivity and cluster packing fraction; see J. M. Ziman, *Models of Disorder* (Cambridge University Press, Cambridge, 1979), p. 380.

³⁶C. Mathioudakis, G. Kopidakis, P. Patsalas, and P. C. Kelires, *Diamond Relat. Mater.* **16**, 1788 (2007).

³⁷H. He and M. F. Thorpe, *Phys. Rev. Lett.* **54**, 2107 (1985).

³⁸Note that the NRL/TB methodology overestimates the bulk modulus of diamond by $\sim 8\%$.